This is a preprint, the final version is subject to change, of the American Mineralogist (MSA)
Cite as Authors (Year) Title. American Mineralogist, in press.
(DOI will not work until issue is live.) DOI: http://dx.doi.org/10.2138/am-2016-5764

REVISION 1

In situ X-ray observation of 10Å phase stability at high pressure

SERGEY V. RASHCHENKO[1,2,3]*, SEIJI KAMADA[4], NAOHISA HIRAO[5], KONSTANTIN D. LITASOV[1,2], EIJI OHTANI[1,4]

[1]SOBOLEV INSTITUTE OF GEOLOGY AND MINERALOGY SB RAS, 3 KOPTYUGA AVE., 630090 NOVOSIBIRSK, RUSSIA

[2]NOVOSIBIRSK STATE UNIVERSITY, 2 PIROGOVA ST., 630090 NOVOSIBIRSK, RUSSIA

[3]INSTITUTE OF SOLID STATE CHEMISTRY AND MECHANOCHEMISTRY SB RAS, 18 KUTATELADZE STR., 630128 NOVOSIBIRSK, RUSSIA

[4]GRADUATE SCHOOL OF SCIENCE, TOHOKU UNIVERSITY, SENDAI 980-8578, JAPAN

[5]JAPAN SYNCHROTRON RADIATION RESEARCH INSTITUTE, KOUTO 1-1-1, SAYO-CHO, SAYO-GUN, HYOGO 679-5198, JAPAN

*Corresponding author e-mail: rashchenko@igm.nsc.ru

ABSTRACT

The 10Å phase, $Mg_3Si_4O_{10}(OH)_2 \cdot H_2O$, is a high-pressure hydrous phyllosilicate considered as an important link in the succession of hydrous phases transporting water into the deep mantle. In this study, in situ synchrotron X-ray diffraction combined with external heating diamond-anvil cell was used to determine limits of the 10Å phase stability at pressures above 7 GPa. A reaction *'10Å phase + H_2O → hydroxide-perovskite (3.65Å phase) + stishovite'* at about 10 GPa was found to be a high-pressure boundary of the 10Å phase stability field. A dehydration temperature of the 10Å phase *'10Å phase → enstatite + stishovite + H_2O'* decreases with pressure from 690°C at 7 GPa to 450°C at 10 GPa; a nonvariant point where 10Å phase, hydroxide-perovskite

and enstatite coexist in the presence of stishovite and hydrous fluid was found near 10 GPa and 450°C.

KEYWORDS: 10Å phase, 3.65Å phase, hydroxide-perovskite, DHMS, deep water cycle

INTRODUCTION

A number of observations, such as electrical conductivity anomalies in the mantle transition zone (MTZ) (e.g., Koyama et al., 2006), seismic evidences of dehydration melting beneath MTZ (Schmandt et al. 2014), or finding of a hydrous ringwoodite inclusion in an ultra-deep diamond (Pearson et al. 2014) convincingly show that MTZ, at least locally, is hydrated. The latter requires an effective mechanism of recycling of surface water to the deep mantle in the cold subduction settings (Ohtani 2015). The most important water reservoir in the subducting slab is serpentinized peridotite of its bottom part (Faccenda et al. 2009), because of (1) higher absolute water content than in sedimentary and gabbro-basaltic layers (Rupke et al. 2004), and (2) cooler geotherm of the slab Moho surface compared with slab – mantle wedge interface favorable for water preservation (Syracuse et al. 2010).

Due to limited temperature stability, serpentine cannot transport H_2O to the deep mantle. However, it can be transformed to dense hydrous magnesium silicates (DHMS) stable at mantle conditions. A commonly considered scheme of water transport to the MTZ implies a successive transformations *'serpentine → phase A, $Mg_7Si_2O_8(OH)_6$ → phase E, $Mg_{2.3}Si_{1.25}H_{2.4}O_6$ → hydrous wadsleyite → hydrous ringwoodite'* (Litasov and Ohtani 2003; Ohtani et al. 2004). In this scheme, the range of subduction geotherms suitable for water transport to the mantle is limited by intersection point of serpentine and phase A dehydration curves, ~ 6 GPa at 600°C (Schmidt and Poli 1998). Such conditions, however, can be achieved only in extremely cold subduction zones, so the geological scale of this process remains questionable (Fig. 1).

This is a preprint, the final version is subject to change, of the American Mineralogist (MSA)
Cite as Authors (Year) Title. American Mineralogist, in press.
(DOI will not work until issue is live.) DOI: http://dx.doi.org/10.2138/am-2016-5764

REVISION 1

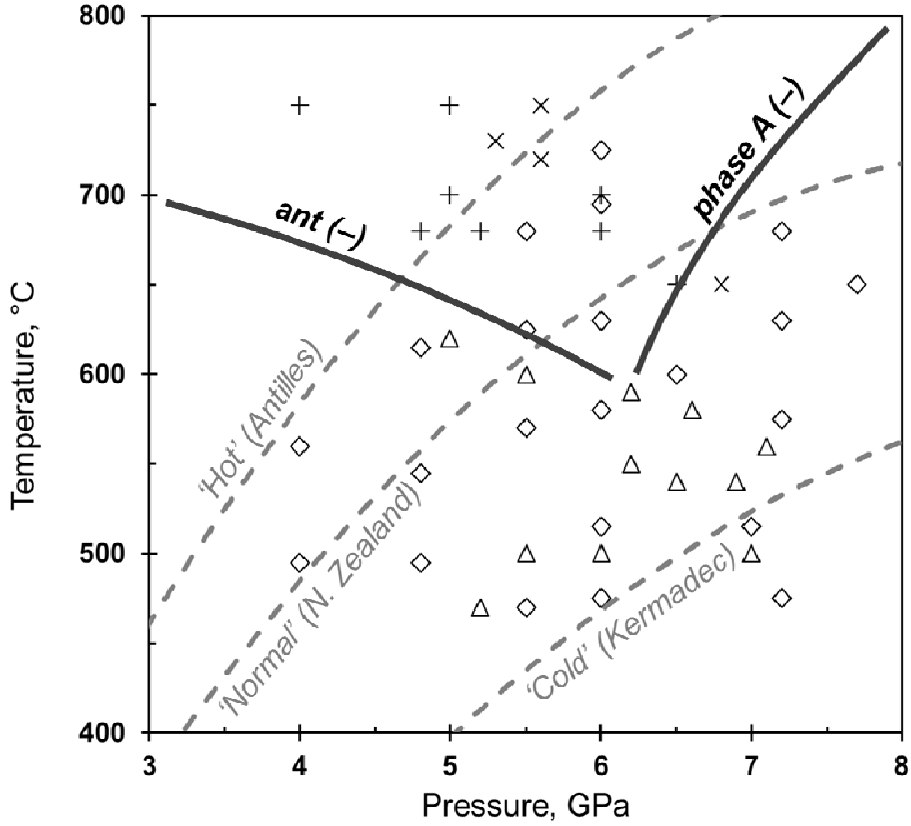

Figure 1. Stability of low-temperature hydrous phases (*ant* – antigorite) in serpentinized peridotite after Schmidt and Poli (1998). The Moho geotherms in subducting slab for Antilles, New Zealand and Kermadec after Syracuse et al. (2010) are shown as examples of 'hot', 'normal' and 'cold' subduction, respectively. *P-T* conditions of experiments with 10 Å phase among run products are shown as diamonds (Yamamoto and Akimoto 1977; Welch et al. 2006 –synthesized from oxides/hydroxides in pure MgO-SiO_2-H_2O (MSH) system), triangles (Ulmer and Trommsdorff 1995; Khodyrev and Agoshkov 1986 – from natural serpentine), '×' (Pawley and Wood 1995 – from natural talc), and '+' (Fumagalli and Poli 2005; Dvir et al. 2011 – from gel with peridotite composition).

Another scheme, described in Schmidt and Poli (2014) involves such DHMS as '10Å phase', $Mg_3Si_4O_{10}(OH)_2 \cdot H_2O$, a phyllosilicate with talc-type layers intercalated by water molecules named accordingly with its d_{001} value (~10Å compared with ~9Å in talc) (Fumagalli et al. 2001; Comodi 2005; Comodi et al. 2006, 2007). Experimental data suggest that the 10Å phase is stable in the 'low temperature gap' between dehydration curves of serpentine and phase A (Fig. 1), and the succession of hydrous phases *'serpentine → 10Å phase → phase A'* can retain about 25% of

H_2O initially stored in the serpentinized peridotite (Schmidt and Poli 2014) even along 'normal' subduction geotherm (Fig. 1).

The dehydration of the 10Å phase limits its stability field by temperature:

$Mg_3Si_4O_{10}(OH)_2{\cdot}H_2O$ (10Å phase) → $3MgSiO_3$ (enstatite) + SiO_2 (coesite / stishovite) + $2H_2O$ (1)

Pawley et al. (2011) studied this reaction between 5 and 7 GPa (in the coesite stability field) and found that it proceeds at 690°C independently on the pressure applied. However, at higher pressures the slope of the given reaction has to change because of *coesite → stishovite* transition.

A low-pressure limit of the 10Å phase stability corresponds to the reaction (2) taking place at ~5 GPa and studied *in situ* by Chinnery et al. (1999) and Rashchenko et al. (2016):

$Mg_3Si_4O_{10}(OH)_2 + H_2O \rightarrow Mg_3Si_4O_{10}(OH)_2{\cdot}H_2O$ (10Å phase) (2)

This reaction actually represents an intercalation of water molecules into the interlayer space of talc.

A high-pressure limit of the 10Å phase is poorly understood. Pawley et al. (2011) reported that decomposition of the 10Å phase near 10 GPa can be associated with formation of the so-called 3.65Å phase, whose composition, $MgSi(OH)_6$, and hydroxide-perovskite structure were determined later (Wunder et al. 2011):

$3Mg_3Si_4O_{10}(OH)_2{\cdot}H_2O$ (10Å phase) → $2MgSi(OH)_6$ (3.65Å phase) + $7MgSiO_3$ (enstatite) + $3SiO_2$ (stishovite) in dry conditions (3),

and $Mg_3Si_4O_{10}(OH)_2{\cdot}H_2O$ (10Å phase) + $7H_2O$ → $3MgSi(OH)_6$ (3.65Å phase) + SiO_2 (stishovite) at $a[H_2O] = 1$ (4)

We used *in situ* synchrotron X-ray diffraction combined with high-temperature diamond-anvil cell to study phase equilibria, which restrict the stability field of the 10Å phase, and constrain the

position of nonvariant point where the 10Å phase, 3.65Å phase and enstatite coexist in the presence of hydrous fluid.

EXPERIMENTAL

Natural talc from Shabrovskoye deposit (Central Ural) with $Mg_{2.94}Fe_{0.05}Al_{0.05}Si_{3.97}O_{10}(OH)_2$ stoichiometry (X-ray fluorescence analysis) was used as a starting material. The talc flakes and a small piece of gold as a pressure standard were placed in a 100 μm hole in a rhenium gasket filled with distilled water. High-pressure – high-temperature conditions were achieved in an external heating diamond anvil cell (DAC) with 600 μm culets and molybdenum resistive heater (Bassett et al. 1993).

Phase transformations in the sample were studied by *in situ* synchrotron X-ray diffraction at BL10XU beamline of SPring-8 synchrotron radiation facility (Hyogo, Japan). An X-ray beam with λ = 0.41468 Å monochromatized with Si (111) double crystal and focused with compound X-ray refractive lenses was used in combination with an image plate (IP) detector (Rigaku RAXIS-IV).

The sample temperature was controlled by an S-type (Pt/Rh 90%/10% – Pt) thermocouple mounted at each anvil near the gasket. The difference between thermocouples readings not exceeded ±1°C, and a deviation of sample temperature from that measured by thermocouples for this type of DAC is believed to be within ±1.5°C (Bassett et al. 1993). Each temperature increment during the experiment was accompanied by a corresponding pressure increase due to the sample thermal pressure and *vice versa*. Several times during the experiment the occurred pressure was corrected to the desired value using control screws. The pressure was measured using equation of state of gold from Sokolova et al. (2013) with uncertainty of ±0.1 GPa. The P-T-t scheme of the experiment is given in Table 1.

Table 1. *P-T-t* scheme of the experiment. '+' – phase detected, '–' – phase absent; phases in minor amount are given in brackets.

Observation #	Time, min	P, GPa	T, °C	talc / 10Å phase	3.65Å phase	enstatite	stishovite
First run							
1	0	3.2	25	+	–	–	–
2	65	5.4	100	+	–	–	–
3	95	8.6	200	+	–	–	–
4	125	10.7	300	+	–	–	–
5	150	11.9	400	+	(+)	–	(+)
6	185	9.7	500	(+)	+	–	+
7	280	9	500	+	–	–	+
8*	0	8.9	500	+	–	–	+
9	80	11.9	550	–	(+)	+	+
10	150	11.7	500	+	+	+	+
11	185	11.4	450	+	+	+	+
Second run							
1a	0	5.7	300	+	–	–	–
2a	85	10.3	450	+	+	–	+
3a	115	12.0	500	+	+	–	+
4a	145	10.5	500	(+)	+	+	+
5a	175	9.3	500	(+)	(+)	+	+
6a	215	10.4	550	–	–	+	+

*After the 7th observation the DAC was cooled from 500°C to ambient temperature without decompression due to a beam shutdown. Then, after ~27 hours, *P-T* conditions were restored (observation #8) and experiment continued.

RESULTS

REVISION 1

The initial mixture of talc and water was pressurized to 3.2 GPa at room temperature. Due to a preferred orientation of talc flakes perpendicular to X-ray beam, all corresponding IP diffraction images show evident heterogeneity of the Debye rings (e.g. Fig. 2, obs. #5). The heating to 400°C during 2.5 hours led to pressure increase to 11.9 GPa. Although talc becomes unstable in the presence of water above 5 GPa (Chinnery et al. 1999), the formation of the 10Å phase started at 11.9 GPa / 400°C only, due to relatively fast heating rate (Fig. 3). The latter agrees with results of Rashchenko et al. (2016), who reported that formation of the 10Å phase from *talc + water* mixture at 8 GPa / 500°C requires at least 2 hours.

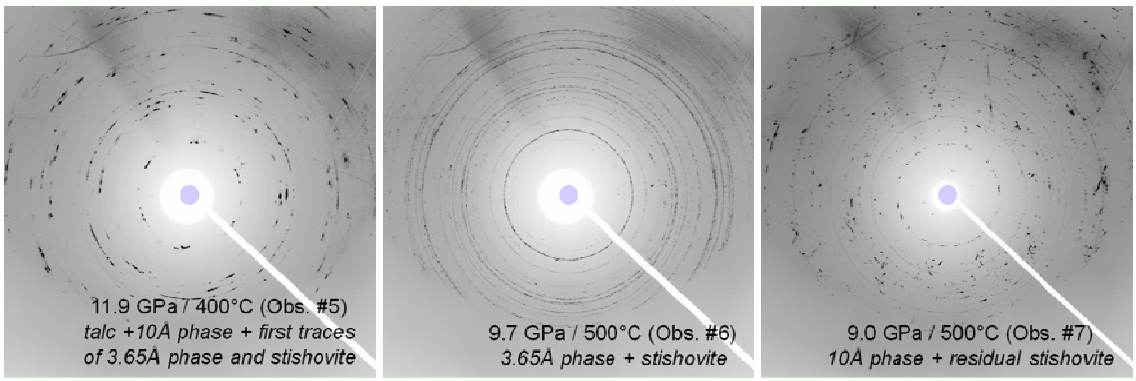

Figure 2. IP diffraction images of different observations of the sample.

This is a preprint, the final version is subject to change, of the American Mineralogist (MSA)
Cite as Authors (Year) Title. American Mineralogist, in press.
(DOI will not work until issue is live.) DOI: http://dx.doi.org/10.2138/am-2016-5764

REVISION 1

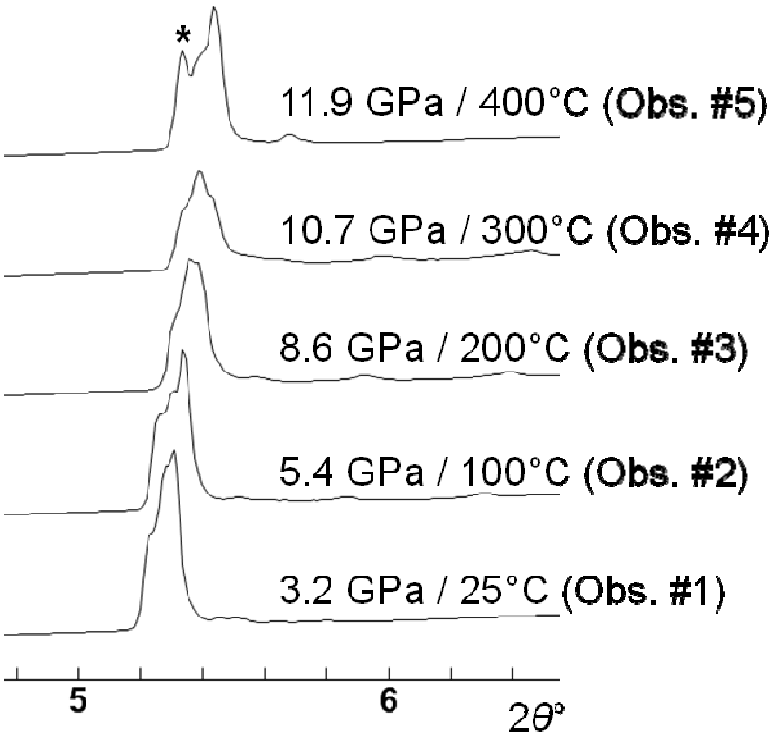

Figure 3. Behavior of multiplet (002 / 020 / 1–10 / 110) X-ray diffraction peak of talc. The separation of (002) peak marked by asterisk at 11.9 GPa / 400°C indicates anisotropic increase of *c* dimension. The latter corresponds to formation of the 10Å phase, a product of water intercalation into talc interlayer space.

Besides the splitting of talc diffraction peaks due to formation of the 10Å phase, a group of new peaks, corresponding to '3.65Å phase' ($MgSi(OH)_6$ hydroxide-perovskite) and stishovite, was also observed at 11.9 GPa / 400°C (Fig. 4). The latter conditions therefore corresponds to the stability field of 3.65Å phase, whereas the formation of the 10Å phase at such conditions should be considered as metastable.

This is a preprint, the final version is subject to change, of the American Mineralogist (MSA)
Cite as Authors (Year) Title. American Mineralogist, in press.
(DOI will not work until issue is live.) DOI: http://dx.doi.org/10.2138/am-2016-5764

REVISION 1

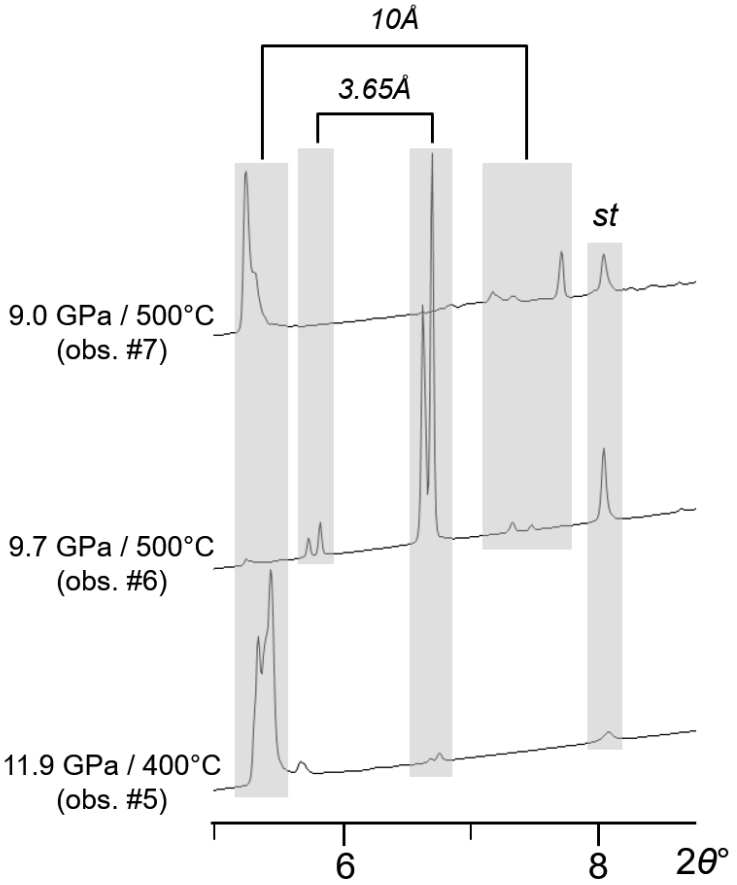

Figure 4. Transformation of metastable talc and 10Å phase (obs. #5) into 3.65Å phase + stishovite (obs. #6) and back to the 10Å phase (obs. #7).

Just after the first peaks of the 3.65Å phase and stishovite were observed, a temperature was increased to 500°C and within 35 min the sample transformed into the mixture of 3.65Å phase and stishovite according to the reaction (4). The newly formed phases demonstrated absence of texturing in contrast to initial talc flakes (Fig. 2, obs. #6). A negative volume effect of the reaction accompanied by gasket relaxation at high temperature led to the pressure decrease from 11.9 to 9.7 GPa, bringing the sample back to the stability field of 10Å phase, and the next observation (#7) showed the complete reverse transformation of *3.65Å phase* + *stishovite* into *10Å phase* + H_2O. An interesting feature of observed phase transformation is the presence of residual stishovite in the sample (5-10 wt. % of stishovite + 90-95 wt. % of 10Å phase) even after complete disappearance of the 3.65Å phase. The latter can be attributed to the formation of

Si vacancies in the 10Å phase by hydrogarnet-type substitution $[SiO_4]^{4-} + 2H_2O \rightarrow [\square(OH)_4]^{4-} + SiO_2$, described in Welch et al. (2006).

Before starting the next experimental run, the sample was cooled down to room temperature and after ~27 hours brought back to 500°C / 8.9 GPa (obs. #8). No changes in phase composition of the sample were observed; the Debye rings became more uniform (Fig. 5).

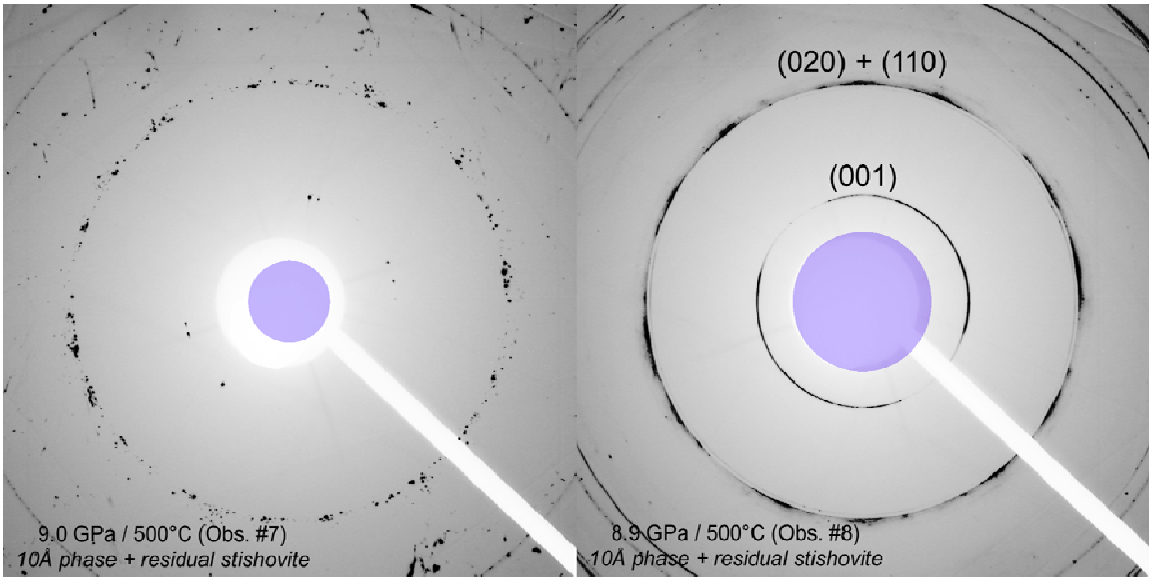

Figure 5. Textural changes in X-ray diffraction pattern of the sample consisting of 10Å phase, residual stishovite, and water fluid after cooling and heating back to 500°C.

To study the temperature limit of the 10Å phase stability at high pressures, we continued heating to 550°C. The observation #9, corresponding to 11.9 GPa / 550°C showed that in about an hour the 10Å phase completely decomposed to assemblage of enstatite and stishovite according to the reaction (1) (Fig. 6a):

$Mg_3Si_4O_{10}(OH)_2 \cdot H_2O$ (10Å phase) → $MgSiO_3$ (enstatite) + SiO_2 (stishovite) + H_2O (1)

A subsequent cooling resulted in growth of the 3.65Å phase (Fig. 6a). The second experimental run performed with the same starting material allowed to better constrain the discussed equilibria (Fig. 6b).

This is a preprint, the final version is subject to change, of the American Mineralogist (MSA)
Cite as Authors (Year) Title. American Mineralogist, in press.
(DOI will not work until issue is live.) DOI: http://dx.doi.org/10.2138/am-2016-5764

REVISION 1

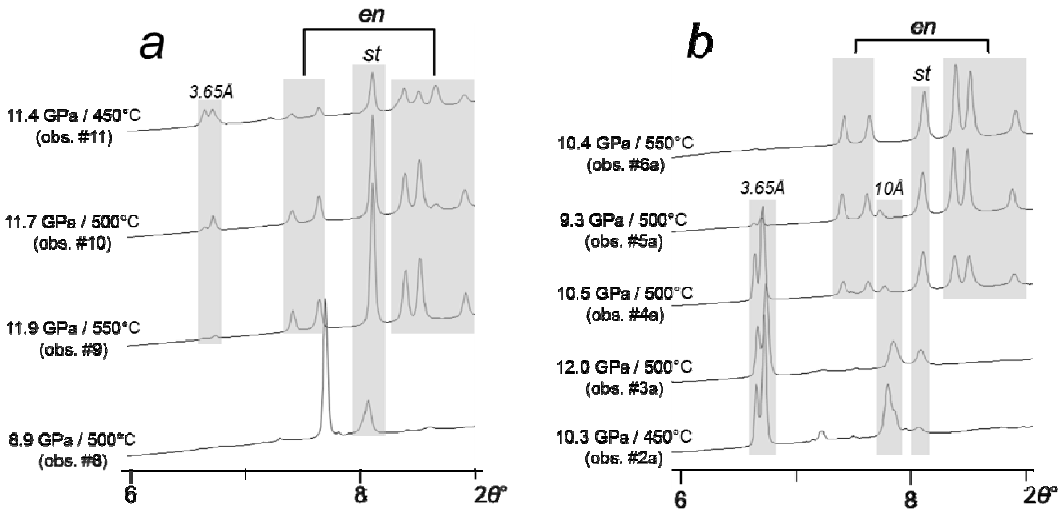

Figure 6. Phase relations between 10Å phase, enstatite, and 3.65Å phase.

Although multiple phases were detected in the most of in situ observations, the changes in the relative intensities of XRD peaks allowed us to constrain the stability fields of the studied phases (Fig. 7). The estimated *PT*-conditions of the non-variant point, where 10Å phase, enstatite, and 3.65Å phase coexist in the presence of stishovite and hydrous fluid, are 10±1 GPa and 450±25°C. The temperature of the 10Å phase dehydration (reaction 1) therefore drops from 690°C at 5-7 GPa to 450°C at 10 GPa indicating that higher pressure does not stabilize this hydrous phase at higher temperatures even in the presence of hydrous fluid, in contrast with such DHMS as phase A (Komabayashi et al. 2005).

This is a preprint, the final version is subject to change, of the American Mineralogist (MSA)
Cite as Authors (Year) Title. American Mineralogist, in press.
(DOI will not work until issue is live.) DOI: http://dx.doi.org/10.2138/am-2016-5764

REVISION 1

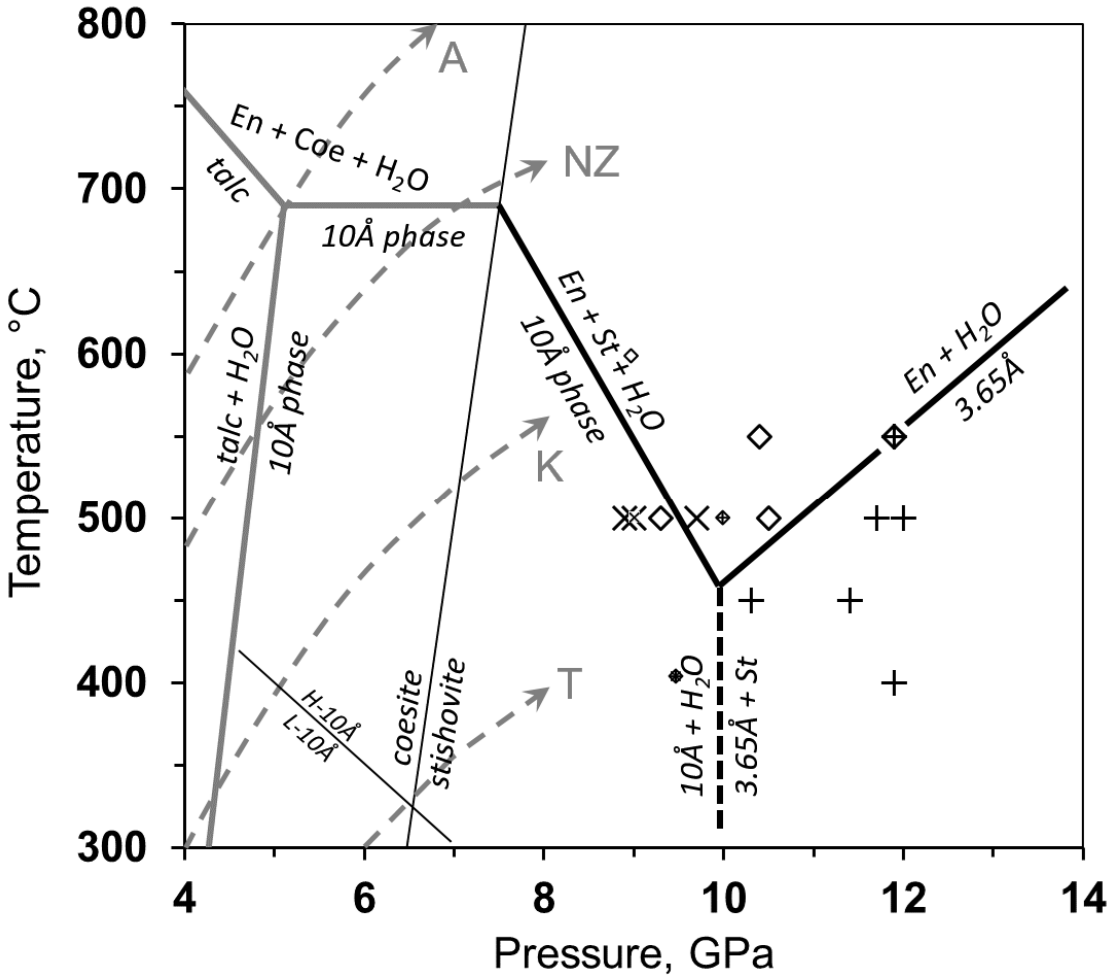

174

175 **Figure 7.** Stability field of the 10Å phase. Gray lines – data from previous works (Pawley and Wood 1995;
176 Chinnery et al. 1999; Pawley et al. 2011), black lines – data from this study. '×', '+' and diamonds correspond to the
177 conditions of 10Å phase, 3.65Å phase, and enstatite *growth*, respectively. Small symbols corresponds to observation
178 of Pawley et al. 2011. A structural transformation of the 10Å phase observed spectroscopically by Comodi et al.
179 (2006, 2007) is shown as H-10Å / L-10Å. The Moho geotherms in subducting slab for Antilles (A), New Zealand
180 (NZ), Kermadec (K) and Tonga (T) after Syracuse et al. (2010) are shown as examples of 'hot', 'normal', 'cold' and
181 'ultracold' subduction, respectively.

182 The high-pressure limit of the 10Å phase stability in the presence of hydrous fluid correspond
183 to the reaction (4) producing $MgSi(OH)_6$ hydroxide-perovskite (3.65Å phase) and stishovite:

184 $Mg_3Si_4O_{10}(OH)_2 \cdot H_2O$ (10Å phase) + $7H_2O \rightarrow 3MgSi(OH)_6$ (3.65Å phase) + SiO_2 (stishovite)
185 (4)

186

187 **IMPLICATIONS**

188 *1. Geological significance of the 10Å phase*

189 Positions of different modern subduction geotherms in relation to the stability field of the 10Å
190 phase (Fig. 7) constrain PT-ranges where the 10Å phase can exist in a subducting slab. The 'hot'
191 subduction geotherm (A) lies outside the 10Å phase stability field. Therefore *pure* 10Å phase
192 cannot be an equilibrium phase in the 'hot' subduction setting. An intermediate temperature
193 geotherm (NZ) crosses the 10Å phase stability field between 5 and 7 GPa, indicating that at 150-
194 225 km the 10Å phase is a potential water reservoir of the subducting slab. Along a 'cold'
195 subduction geotherm (K) the 10Å phase can exist in a wide pressure range of 4-9 GPa
196 corresponding to 125-275 km depths. A dehydration of the 10Å phase below 275 km may be
197 responsible for the deep seismicity of the lower part of double seismic zones.

198 We should also note that the discussed stability field actually corresponds to the silica-rich
199 *'talc/10Å phase + H_2O'* system with Mg:Si ratio of 3:4. The subducting serpentinized peridotite
200 contains less silica (Mg:Si > 1:1), and subducted water can be also retained in such Mg-rich
201 phases as serpentine and phase A, $Mg_7Si_2O_8(OH)_6$, whose stability fields partly overlap the
202 stability field of the 10Å phase. Nevertheless, Ulmer and Trommsdorff (1999) after thorough
203 review of existed experimental data on serpentinized peridotites underlined that *'the 10Å phase*
204 *forms part of the stable phase assemblage in a PT-interval between 5.5 and 7.5 GPa just above*
205 *the antigorite breakdown'*. On the other hand, the presence of Al_2O_3 and K_2O can significantly
206 broaden the stability field of pure 10Å phase (Fumagalli and Poli 2005; Fumagalli et al. 2009;
207 Dvir et al. 2011). The latter explains experimental observations of the 10Å phase above the

208 temperature of its pure end-member decomposition (690°C) – see Fig. 1, and also broadens the
209 range of geotherms suitable for the 10Å phase formation.

210 *2. Geological significance of the $MgSi(OH)_6$ hydroxide-perovskite (3.65Å phase)*

211 Although the 3.65Å phase was first reported decades ago in short conference abstracts of
212 Sclar and Morzenti (1971) and Rice et al. (1989), its $MgSi(OH)_6$ composition and an A-vacant
213 perovskite structure of this the most H_2O-rich DHMS were determined only recently (Wunder et
214 al. 2011, 2012; Welch and Wunder 2012; Mookherjee et al. 2015). The low temperature stability
215 of the 3.65Å phase makes it unrealistic for the most of subduction geotherms (Fig. 7). However,
216 the position of Moho geotherm of Tonga subduction zone, which is the coldest geotherm
217 according to Syracuse et al. (2010) (Fig. 6), allows us to suggest that a succession *'serpentine →*
218 *10Å phase → 3.65Å phase'* can lead to formation of the $MgSi(OH)_6$ hydroxide-perovskite at
219 depths below 300 km. The presence of aluminum may probably extend the temperature stability
220 of the $MgSi(OH)_6$, similar to that shown for $Mg^{2+}Si^{4+} \leftrightarrow 2Al^{3+}$ substitution in a high-pressure
221 phase D, $MgSi_2O_4(OH)_2$ (Ohira et al. 2014; Pamato et al. 2015), and requires a further study.

222 *3. Kinetics of hydrous phases decomposition*

223 We should also note an extreme reactivity of all hydrous phases observed in our experiments.
224 For example, a complete high-pressure breakdown *'10Å phase → 3.65Å phase + stishovite'*
225 (observations #5-6) was observed in 35 minutes only, in contrast to reported syntheses of the
226 3.65Å phase from *'brucite + quartz + water'* mixture (114 h) and gel (77 h) under similar PT-
227 conditions (Wunder et al. 2011). The latter allows us to recommend the 10Å phase (or talc) as a
228 highly reactive starting material for high-speed synthesis of DHMS. The fast kinetics of the
229 observed reactions also allowed us successfully implement synchrotron-based in situ XRD
230 coupled with high-temperature DAC for real-time observation of forward and backward
231 reactions in the studied system. Such an approach (although requiring a fact kinetics) seems very

perspective for petrological investigations instead of time-consuming routine quenching experiments.

ACKNOWLEDGEMENTS

The research was supported by state assignment project #0330-2016-004, Russian Ministry of Education and Science [grant #14.B25.31.0032], Russian Science Foundation [grant #14-13-00834], and Japan Society for the Promotion of Science [grants ##22000002 and 15H5748]. The in situ synchrotron X-ray diffraction experiments were performed under SPring-8 research proposals ##2014B0104 and 2015B0104. We acknowledge F. Maeda, N. Suzuki and R. Masudo for their kind assistance in preparation of this experiment.

REFERENCES

Bassett, W.A., Shen, A.H., Bucknum, M., Chou, I-M. (1993) A new diamond anvil cell for hydrothermal studies to 2.5 GPa and from −190 to 1200°C. Review of Scientific Instruments, 64, 2340-2345.

Chinnery, N.J., Pawley, A.R., and Clark, S.M. (1999) In situ observation of the formation of 10Å phase from talc + H_2O at mantle pressures and temperatures. Science, 286, 940-942.

Comodi, P. (2005) The 10 Å phase: Crystal structure from single-crystal X-ray data. American Mineralogist, 90, 1012-1016.

Comodi, P., Cera, F., Dubrovinsky, L., and Nazzareni, S. (2006) The high-pressure behaviour of the 10 Å phase: A spectroscopic and diffractometric study up to 42 GPa. Earth and Planetary Science Letters, 246, 444-457.

Comodi, P., Cera, F., Nazzareni, S., and Dubrovinsky, L. (2007) Raman spectroscopy of the 10Å phase at simultaneously H*P*-H*T*. European Journal of Mineralogy, 19, 623-629.

Dvir, O., Pettke, T., Fumagalli, P., and Kessel, R. (2011) Fluids in the peridotite–water system up to 6 GPa and 800°C: New experimental constrains on dehydration reactions. Contributions to Mineralogy and Petrology, 161, 829-844.

Faccenda, M., Gerya, T.V., and Burlini, L. (2009) Deep slab hydration induced by bending-related variations in tectonic pressure. Nature Geoscience, 2, 790-793.

Fumagalli, P., Stixrude, L., Poli, S., and Snyder, D. (2001) The 10 Å phase: A high-pressure expandable sheet silicate stable during subduction of hydrated lithosphere. Earth and Planetary Science Letters, 186, 125-141.

Fumagalli, P. and Poli, S. (2005) Experimentally determined phase relations in hydrous peridotites to 6.5 GPa and their consequences on the dynamics of subduction zones. Journal of Petrology, 46, 555-578.

Fumagalli, P., Zanchetta, S., and Poli, S. (2009) Alkali in phlogopite and amphibole and their effects on phase relations in metasomatized peridotites: a high-pressure study. Contributions to Mineralogy and Petrology, 158, 723–737.

Khodyrev, O.Y. and Agoshkov, V.M. (1986) Phase transformations of serpentine in the system MgO-SiO_2-H_2O at the pressure range 40 to 80 kbar. Geokhimiya, 264-269.

Komabayashi, T., Hirose, K., Funakoshi, K., and Takafuji N. (2005) Stability of phase A in antigorite (serpentine) composition determined by in situ X-ray pressure observations. Physics of the Earth and Planetary Interiors, 151, 276-289.

Koyama, T., Shimizu, H., Utada, H., Ichiki, M., Ohtani, E., Hae, R. (2006) Water content in the mantle transition zone beneath the North Pacific derived from the electrical conductivity

277 anomaly. In: Jacobsen, S.D. and van der Lee, S. (eds.) Earth's Deep Water Cycle. American
278 Geophysical Union, 171-179.

279 Litasov, K., and Ohtani, E. (2003) Stability of various hydrous phases in CMAS pyrolite –
280 H_2O system up to 25 GPa. Physics and Chemistry of Minerals, 30, 147-156.

281 Mookherjee, M., Speziale, S., Marquardt, H., Jahn, S., Wunder, B., Koch-Muller, M., and
282 Liermann, H.P. (2015) Equation of state and elasticity of the 3.65Å phase: Implications for the
283 X-discontinuity. American Mineralogist, 100, 2199-2208.

284 Ohira, I., Ohtani, E., Sakai, T., Miyahara, M., Hirao, N., Ohishi, Y., Nishijima, M. (2014)
285 Stability of a hydrous δ-phase, AlOOH-$MgSiO_2(OH)_2$, and a mechanism for water transport into
286 the base of lower mantle. Earth and Planetary Science Letters, 401, 12-17.

287 Ohtani, E., Litasov, K., Hosoya, T., Kubo, T., and Kondo, T. (2004) Water transport into the
288 deep mantle and formation of a hydrous transition zone. Physics of the Earth and Planetary
289 Interiors, 143, 255-269.

290 Ohtani, E. (2015) Hydrous minerals and the storage of water in the deep mantle. Chemical
291 Geology, 418, 6-15.

292 Pamato, M.G., Myhill, R., Ballaran, T.B., Frost, D.J., Heidelbach, F., Miyajima, N. (2015)
293 Lower-mantle water reservoir implied by the extreme stability of a hydrous aluminosilicate.
294 Nature Geoscience, 8, 75-79.

295 Pawley, A.R. and Wood, B.J. (1995) The high-pressure stability of talc and 10Å phase –
296 potential storage sites for H_2O in subduction zones. American Mineralogist, 80, 998-1003.

297 Pawley, A.R., Chinnery, N.J., Clark, S.M., and Walter, M.J. (2011) Experimental study of the
298 dehydration of 10Å phase, with implications for its H_2O content and stability in subducted
299 lithosphere. Contributions to Mineralogy and Petrology, 162, 1279-1289.

Pearson, D.G., Brenker F.E., Nestola F., McNeill J., Nasdala L., Hutchison M.T., Matveev S., Mather K., Silversmit G., Schmitz S., Vekemans B., and Vincze L. (2014) Hydrous mantle transition zone indicated by ringwoodite included within diamond. Nature, 507, 221-224.

Rashchenko, S.V., Likhacheva, A.Yu., Goryainov, S.V., Krylov, A.S., and Litasov K.D. (2016) In situ spectroscopic study of water intercalation into talc: New features of 10Å formation. American Mineralogist, 101, 431–436.

Rice, S.B., Benimoff, A.I., and Sclar, C.B. (1989) "3.65 Å phase" in the system MgO-SiO_2-H_2O at pressures greater than 90 kbars. Crystallochemical implications for mantle phases. International Geological Congress, Washington, D.C., 2, 69.

Rupke, L.H., Morgan J.P., Hort M., and Connolly J.A.D. (2004) Serpentine and the subduction zone water cycle. Earth and Planetary Science Letters, 223, 17-34.

Schmandt, B., Jacobsen, S.D., Becker, T.W., Liu Z.X., and Dueker K.G. (2014) Dehydration melting at the top of the lower mantle. Science, 344, 1265-1268.

Schmidt, M.W. and Poli, S. (1998) Experimentally based water budgets for dehydrating slabs and consequences for arc magma generation. Earth and Planetary Science Letters, 163, 361-379.

Schmidt, M.W. and Poli, S. (2014) Devolatilization during subduction. In: Holland, H.D. and Turekian, K.K. (eds.) Treatise on Geochemistry (2nd edition). Amsterdam, Netherlands: Elsevier, 669-701.

Sclar, C.B. and Morzenti, S.P. (1971) High pressure synthesis and geophysical significance of a new hydrous phase in the system MgO-SiO_2-H_2O. Geological Society of America Abstract Programs, 3, 698.

Sokolova, T.S., Dorogokupets, P.I., and Litasov, K.D. (2013) Self-consistent pressure scales based on the equations of state for ruby, diamond, MgO, B2–NaCl, as well as Au, Pt, and other metals to 4 Mbar and 3000 K. Russian Geology and Geophysics, 54, 181-199.

Syracuse, E.M., van Keken P.E., and Abers G.A. (2010) The global range of subduction zone thermal models. Physics of the Earth and Planetary Interiors, 183, 73-90.

Ulmer, P. and Trommsdorff, V. (1995) Serpentine stability to mantle depths and subduction-related magmatism. Science, 268, 858-861.

Ulmer, P. and Trommsdorff, V. (1999) Phase relations of hydrous mantle subducting to 300 km. In: Fei, Y., Bertka, C.M., and Mysen, B.O. (eds.) Mantle Petrology: Field Observations and High Pressure Experimentation. The Geochemical Society, 259-282.

Welch, M.D., Pawley, A.R., Ashbrook, S.E., Mason, H.E., and Phillips, B.L. (2006) Si vacancies in the 10 Å phase. American Mineralogist, 91, 1707-1710.

Welch, M.D. and Wunder, B. (2012) A single-crystal X-ray diffraction study of the 3.65Å phase $MgSi(OH)_6$, a high-pressure hydroxide-perovskite. Physics and Chemistry of Minerals, 39, 693-697.

Wunder, B., Wirth R., and Koch-Muller, M. (2011) The 3.65Å phase in the system MgO-SiO_2-H_2O: Synthesis, composition, and structure. American Mineralogist, 96, 1207-1214.

Wunder, B., Jahn, S., Koch-Muller, M., and Speziale, S. (2012) The 3.65Å phase, $MgSi(OH)_6$: Structural insights from DFT-calculations and T-dependent IR spectroscopy. American Mineralogist, 97, 1043-1048.

Yamamoto, K. and Akimoto, S. (1977) The system MgO-SiO_2-H_2O at high pressures and temperatures – stability field for hydroxylchondrodite, hydroxylclinohumite and 10Å phase. American Journal of Science, 277, 288-312.